

## PalArch's Journal of Archaeology of Egypt / Egyptology

Optimization of layout of the large-size wind turbines with horizontal axis in the wind farm

*Alireza SHirzadegan<sup>1</sup>, Reza Aghaei Togh<sup>2\*</sup>*

<sup>1</sup> Ph.D. Student, Department of aerospace Engineering, Islamic Azad University Science and Research Branch, Tehran, Iran, E-mail: alireza.shirzadegan@srbiau.ac.ir

<sup>2</sup> Assistant professor, Department of aerospace Engineering, Islamic Azad University Science and Research Branch, Tehran, Iran, E-mail: reza\_tog@srbiau.ac.ir

\*corresponding author

**Alireza SHirzadegan, Reza Aghaei Togh: Optimization of layout of the large-size wind turbines with horizontal axis in the wind farm -- Palarch's Journal Of Archaeology Of Egypt/Egyptology 18(7), ISSN 1567-214x**

**Keywords: Wind turbine, renewable energy, turbine layout, wind farm, optimization**

### ABSTRACT

The purpose of the study was to provide the best layout of large-size wind turbines so that the highest efficiency could be attained from wind turbines or in other words, the maximum electricity would be generated in a wind farm. The study first examined a single wind turbine and then three wind turbines together. Moreover, V-47 660 KW wind turbine was selected for the study according to the analyses performed. This study was done numerically in CFX software. The study also used the blade element method (BEM). It has to be noted that the BEM theory was used for aerodynamic calculations of wind turbine blades. Finally, according to the information obtained from the analysis of these three wind turbines together and the output power extracted from these turbines, the best layout of wind turbines in a wind farm was obtained. If this layout is used in wind farms the most power generated from wind turbines can be obtained.

### 1. INTRODUCTION

Nowadays, everyone is aware of the need to replace fossil fuels. Some countries lacking fossil fuel resources have a higher incentive to replace fossil fuels with other resources and have been more pioneering than others. Overall, by replacing wind energy with wind power from fossil fuel power plants, one can reduce greenhouse gas emissions. On the other hand, the natural attractions and landscapes of wind energy systems are considered a symbol of clean energy for people [1]. Moreover, 99% of the land allocated to wind farm construction can be used for agricultural and livestock activities and only about 1% is used by turbines. Power generation forms only one part of a country's energy. Thus, wind force alleviates the negative effects. Since wind can replace fuel for electricity generation, wind power can alleviate global warming. Additionally, unlike fossil or nuclear power plants that use large volumes of water to cool facilities, wind turbines do not need water to generate electricity. At the moment, the largest capacity of installed wind turbines in recent decades

has been the grid-connected type. Nonetheless, sometimes grid-disconnected wind turbines are used in remote areas as well. Most of the wind turbines start electricity generation when the wind velocity is about 3 to 4 meters per second, producing a maximum allowable power of about 15 m/s [2]. In today's world, many wind turbines have been installed and operated. These turbines have been produced in various generations and completed over time. Wind power generation capacity quadrupled from 2000 to 2006. It could be stated that wind power generation doubles every three years. In countries like Denmark and Spain, which have been forerunners in this regard, more than 10% of their electricity is generated by wind, and about 81% of wind turbines are installed in the United States and Europe [3].

There is restricted predictability for the output of wind farms considering the changes in wind. Wind must be programmable like other energy sources. Nevertheless, the nature of the wind renders the phenomenon variable inherently. Although some approaches are used to predict the power generation of these power plants, the predictability of these power plants is overall low. These power plant problems are usually partially eliminated by using energy storage approaches like using pumped water power plants. Wind resources are wind farm fuel, and small changes have major effects on its commercial value. Therefore, even small changes in average wind velocity can make a big difference in efficiency. Some information obtained from studying the wind technology market in Germany as a leader in the world wind industry shows the trend of developments in recent years in this industry, attention to which will be useful in predicting the future. The average capacity of wind turbines installed in Germany is about 1000 kWh. However, if we consider only the turbines installed in the first half of 2007, the average capacity of new wind turbines is about twice this value. Hence, a clear trend of increasing the size of modern wind turbines is observed [4].

A paper entitled "Wind Turbine Blade Design Optimization" in MIT University in April 2010 studied and analyzed the geometric shape of the turbine blade using the control screw method and considering wind velocity changes [5]. The method is designed and tested for a right angle layout. They have tried to maximize the output energy while minimizing the blade volume and destructive pressures on it using genetic algorithm. Given the results from DOE and SQP software, the efficiency obtained is between 60 and 70% of the efficiency of Betz's law at the best points.

In July 2011, in Amirkabir University, in their paper entitled "Effects of turbulence model in computational fluid dynamics of horizontal axis wind turbine aerodynamic", Mansour and Yahyazadeh modeled the aerodynamics of horizontal wind turbines numerically using CFD in three various turbulence models [6]. The results from turbulence modeling proved a very high degree of reliability. The blades are located at a screw angle of  $12^\circ$  and the results for various turbulence modes are recorded according to RNG K- $\epsilon$  and SPALART-ALLMARAS standards and compared with experimental data from the National Renewable Energy Laboratory (NREL) for two various velocities. The study revealed that the CFD calculations for the aerodynamics of horizontal axle-based wind turbine blades based on RNG K- $\epsilon$  for low velocities are more consistent

with the experimental data and the SPALART-ALLMARAS model is more in line with the experimental data for high velocities.

Fort and Porte (December 2011) studied the wake in turbulence layers behind the wind turbines and obtained the closest wake in the turbine layers behind the turbine flow in another paper entitled “Wake Measurements Behind an Array of Two Model Wind Turbines.” Moreover, they showed these wakes in some figures (extracted from Fluent software) based on the distance in the direction of wind flow and perpendicular to the wind flow behind the turbine. Additionally, in other figures, by keeping the distance constant in the direction of the wind flow, they changed the distance in the direction perpendicular to the flow in both Y and Z directions, and finally identified the worst states at various distances, suggesting that much better efficiency will be attained if the wake effects from turbulence layers decrease [7]. Hsiao et al. (2013) made a practical test and did a numerical solution in three different states of a blade with NACA 4418 airfoil profile and a diameter of 0.72 meters in another paper entitled “The Performance Test of Three Different Horizontal Axis Wind Turbine (HAWT) Blade Shapes Using Experimental and Numerical Methods.” In the wind tunnel test, the maximum power factor for the blade was 0.42. The same maximum coefficient is used for OPT and UOT modes and various  $\lambda$ s have been reached:  $\Lambda = 4.92$  for OPT mode and  $\lambda = 4.32$  for UOT mode. The maximum power factor obtained for UUT mode at  $\lambda = 3.86$  is 0.21. Numerical solution with CFD method has been done for all three cases with very logical and convergent results in line with those of the practical test after performing the practical test [8].

Considering the practical and theoretical studies on wind turbines and wind energy, one can claim that the main topics of the day related to wind turbines are to increase the efficiency of wind turbines and how to delay the separation in the flow and improve lift and drag ratios. Researchers have done a lot of studies regarding this like examining the distance of turbulent flow to the wind turbine blade, using methods like plasma to delay separation, examining flexible blades and elasticity, analyzing wind turbines in unstable flows, and studying turbulent flow behavior with a wake behind the wind turbine blades, examining the oscillations and vibrations in the wind turbine blades and using tools like vortex generator to delay separation and many other studies. However, what has received more attention in recent years in improving the operating efficiency of wind turbines has been the type of layout of wind turbines in a centralized complex so that besides enhancing the efficiency and output power of the wind turbines, less space is occupied for wind turbine installation, meaning wind turbine optimization, which is very economical.

## 2. METHODS

### 2-1. Selection of wind turbines for windy sites

#### 2-1-1. Specifications of wind turbines

Various environmental conditions affect wind turbines so that these conditions play a key role in the output load and the useful life and operation of turbines. For the optimal choice of turbine type, all environmental and soil parameters have to be taken into account to reach

greater reliability and higher safety factor. Environmental conditions are divided into two subsets: normal winds and high winds. Normal wind conditions have a long-term effect on the loads on the structure and operating conditions, whereas high winds, although rare, can potentially cause critical conditions. Wind turbines are grouped into various classes according to their tolerance and capacity against wind conditions based on IEC 61400-1 Rev2.

These classes are categorized according to the average wind velocity over a ten-minute period, with the probability of higher winds occurring once every 50 years, and the average annual wind velocity at the hub height of the turbine.

**Table 1:** The class of wind turbines according to IEC standard

WT classes	I	II	III	IV
$V_{ref}$ [m/s]	50.0	42.5	37.5	30.0
$V_{ave}$ [m/s]	10.0	8.5	7.5	6.0
$A_{115}$	0.18	0.18	0.18	0.18
$B_{115}$	0.16	0.16	0.16	0.16

The numbers shown in Table 1 are the maximum values for each wind class

$V_{ref}$ : 50-year average wind velocity over a period of 10 minutes

$V_{av}$ : Average annual wind velocity at hub height

A: Determiner of subgroup for high wind characteristics and severe turbulence

B: Determiner of subgroup for high wind characteristics and weak disturbances

$L_{15}$ : Characteristic value of turbulence intensity at a velocity of 15 meters per second

### 2.1.2. High winds

Turbines must be designed so as to withstand high winds. High wind conditions can be classified according to the maximum average wind velocity obtained in a given period. According to the IEC standard, reversible periods are set over a period of 50 years, and the base wind velocity ( $V_{ref}$ ) is the average wind velocity every ten minutes over a period of 50 years.  $V_{ref}$  parameter is specified according to the anemometer operations performed on the site (area) in Wind Pro software.

### 2.1.3. Average annual wind velocity

The average annual wind velocity for hub heights ( $V_{av}$ ) is obtained using various meteorological software and anemometer operations. Generally, besides suitable environmental conditions, other side factors like wind continuity, calculation of wind density, site access conditions (windy area), traffic restrictions, being earthquake prone, soil science, urography (ground and elevation) and even the surface and ground roughness

conditions where the wind turbine is to be installed should also be considered to select and install a wind turbine, because if the surface roughness is high, it can lead to turbulent flow, damage the wind turbine blade structure and reduce the wind turbine output power.

#### 2.1.4. Determining the wind turbine class

Given the above and the values obtained from the velocity of the site and meteorological stations, the 50-year average wind velocity for 10 minutes ( $V_{ref}$ ) and the average annual wind velocity for hub heights ( $V_{ave}$ ) for most windy sites with favorable conditions for installing large size wind turbines with horizontal axis are, respectively,  $V_{ref} = 37.2$  and  $V_{ave} = 8.3$  m/s. According to the information obtained from the velocity values and considering Table 1, the wind turbine class for these windy sites is in Class 2. Wind turbine V47-660 kW has been selected with reference to reputable companies in the production of wind turbines with horizontal axis in large size like Siemens and Vestas. It has to be stated that this wind turbine is the best choice to be used in these windy areas and has the highest efficiency and output power.

#### 2.1.5. Wind turbine simulation

Three-dimensional modeling of one blade of this wind turbine was performed based on the existing two-dimensional drawings of the various components of the V47-660 kW wind turbine. It has to be noted that this wind turbine blade is composed of different sections with different profile shapes. The whole wind turbine with horizontal axis will be modeled completely. The solution amplitude will be defined for three wind turbines. A large rectangular cube is used as the solution amplitude to simulate a field with three turbines. This rectangle is 200 meters wide, 120 meters high and 800 meters long. In this rectangle, 3 discs with a diameter of 47 meters and a thickness of 0.5 meters were placed at a height of 50 meters from the ground, representing the three wind turbines. The whole range is networked using pyramid elements so that it is closer to the turbine disks. Thus, only the wind turbine environment is solved in three dimensions and the wind turbines alone are simulated in two dimensions. Hence, the problems of large solution amplitude and high number of elements were solved and the problem could be solved.

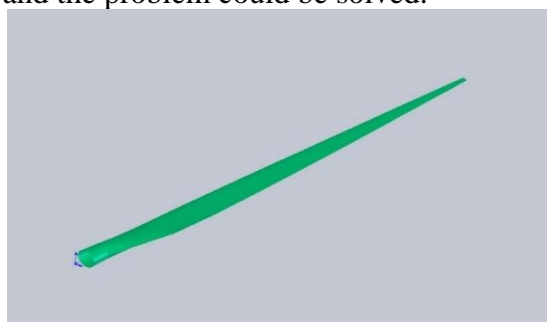


**Figure 1:** Wind turbine V47-660 kW 3D model of blade



**Figure 2:** Wind turbine V47–660 kW 3D model

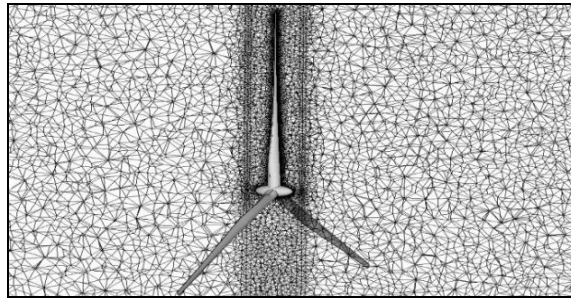


**Figure 3:** Networking for the farm including three V47–660 kW wind turbines

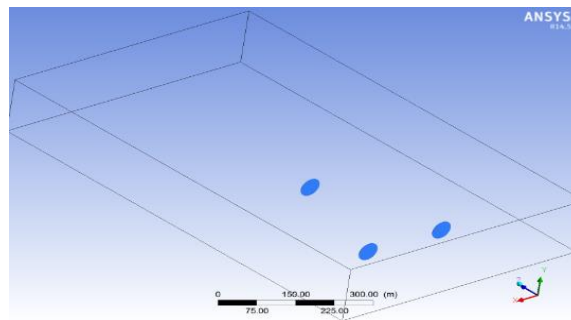


**Figure 4:** Solution range for the farm including three wind turbines

### 2.1.6. Governing equations

It is necessary to solve the continuity and momentum equations to obtain the velocity components in the three directions of the coordinate axes to solve any flow.

#### 2.1.6.1. Continuity equation

The equation of conservation of mass or continuity for smooth flow in the general case and in vector form is written as follows.

$$\frac{\partial \rho}{\partial t} + \nabla \cdot (\rho \vec{v}) = S_m \quad (1)$$

This equation applies for both compressible and incompressible flows. The term  $S_m$  represents the mass added to the continuous phase because of the change of state of the second phase in multiphase flows (like evaporation of liquid droplets and their addition to the gas phase).

#### 2.6.1.2. Momentum equations

Momentum equations are written in an inertial coordinate system (origin of non-acceleration coordinates) for smooth flow as follows:

$$\frac{\partial \rho}{\partial t} (\rho \vec{v}) = \nabla \cdot (\rho \vec{v} \vec{v}) = -\nabla p + \nabla \cdot (\vec{\tau}) + \vec{F} \quad (2)$$

In the above phrase, p is the static pressure and  $\vec{F}$  the volumetric forces applied on the fluid, such as the force of gravity or the forces acting on the liquid phase or phases because of the interaction in a multiphase flow.

**2.1.7. Solution algorithm**

The blade element method (BEM) was used to simulate the turbine two dimensionally. BEM theory is used for aerodynamic calculations of wind turbine blades. Overall, this theory can be used to analyze the existing blade aerodynamically or design it from the start. Momentum theory of elements is obtained by combining two different methods of aerodynamic calculations of wind turbine blades. The first method is to use conservation of momentum equation on the flow through the turbine and the second method is to calculate the lift and drag ratios on different blade sections. A series of equations are obtained that are solved iteratively by combining these two methods.

**2.1.7.1. Two-dimensional wind turbine simulation**

If we consider the flow passing around the turbine as a tunnel, as in Figure 5, four distinct points can be distinguished: 1) upstream, 2) just before the plates containing the blades, 3) just after the plates containing the blades, and 4) downstream. Energy is extracted from the wind flow between points 2 and 3, and thus changes will occur in pressure. Assuming  $p_1 = p_4$  and  $V_2 = V_3$ , meaning that the pressure is the same upstream and downstream, no change in the flow velocity because of the incompressibility of the flow, as well as ignoring the viscosity and friction between points 1 and 2 and points 3 and 4, one can write Bernoulli equation as follows.

$$p_2 - p_3 = \frac{1}{2} \rho (V_1^2 - V_4^2) \quad (3)$$

Considering the force as the product of pressure multiplied by the surface, we will have:

$$dF_x = (p_2 - p_3) dA \quad (4)$$

$$dF_x = \frac{1}{2} \rho (V_1^2 - V_4^2) dA \quad (5)$$

Here, x shows the axial direction. We define parameter a as the axial induction coefficient.

$$a = \frac{V_1 - V_2}{V_1} \quad (6)$$

It is concluded that:

$$V_2 = V_1(1 - a) \quad (7)$$

$$V_4 = V_1(1 - 2a) \quad (8)$$

By placing it in the force equation, it is concluded:

$$dF_x = \frac{1}{2} \rho V_1^2 [4a(1 - a)] 2\pi r dr \quad (9)$$

In fact, this is the axial force acting on a blade element. Now, if we assume the circular flow around the blade plate according to Figure 6, 4 points can be defined as before: : 1) upstream, 2) just before the plates

containing the blades, 3) just after the plates containing the blades, and 4) downstream. The rotation of the blades between points 2 and 3 creates a rotating flow behind the blades. The above equations are written assuming that the flow is two-dimensional so that there is no radial flow. The assumption does not apply to the tip of the blade. Given the end of the blade in this area, the flow tends to go from the high pressure side of the airfoil to the low pressure side. This movement is done from the shortest path - the radial direction. Thus, special vortices are formed in this area and cause losses. These variations can also be calculated for BEM theory and used in the equations by the correction factor. This correction factor (Q), called the Prandtl drop coefficient, differs from 0 to 1 and determines the reduction in the forces acting on the blade.

$$Q = \frac{2}{\pi} \cos^{-1} \left[ \exp \left\{ - \left( \frac{B/2 [1 - r/R]}{(r/R) \cos \beta} \right) \right\} \right] \quad (10)$$

The tip correction factor is used in the equations as follows.

$$dF_x = Q \rho V_1^2 [4a(1-a)] \pi r dr \quad (11)$$

$$dT = Q 4a'(1-a) \rho V_1^2 \Omega r^3 \pi dr \quad (12)$$

Four equations have been obtained so far: two equations from momentum theory stating the axial forces and momentum in terms of flow parameters.

$$dF_x = Q \rho V_1^2 [4a(1-a)] \pi r dr \quad (13)$$

$$dT = Q 4a'(1-a) \rho V_1^2 \Omega r^3 \pi dr \quad (14)$$

Moreover, two equations are obtained from the calculation of axial forces and blade momentum in terms of lift and drag forces.

$$dF_x = \sigma' \pi \rho \frac{V^2 (1-a)^2}{\cos^2 \beta} (C_L \sin \beta + C_D \cos \beta) r dr \quad (15)$$

$$dT = \sigma' \pi \rho \frac{V^2 (1-a)^2}{\cos^2 \beta} (C_L \cos \beta - C_D \sin \beta) r^3 dr \quad (16)$$

The following two functional equations are calculated by equating the equations obtained above.

$$\frac{a}{1-a} = \frac{\sigma' [C_L \sin \beta + C_D \cos \beta]}{4Q \cos^2 \beta} \quad (17)$$

$$\frac{a'}{1-a} = \frac{\sigma' [C_L \cos \beta - C_D \sin \beta]}{4Q \lambda_r \cos^2 \beta} \quad (18)$$

Two-dimensional methods are used to analyze the behavior of wind turbines in this section. A computational code was created to facilitate and increase speed. This code is based on the BEM theory. To this end, the blade must first be divided into finite elements. In each of these elements, the torsion angle, chord size, chord length and type of airfoil used in the element must be specified. This information is entered into the code by a text file. This layout is done at 22 points between the maximum chord radii to the end of the blade. The blade element text file along with the text files containing the drag and lift ratio for different airfoils used in the blade are provided as input to the code. After explaining the code inputs, it has to be noted that the written code has two main parts, including the initial code and the duplicate loop code.

**2.1.7.2. Calculation of lift and drag ratios**

To reach the desired answers in two-dimensional simulation, the lift and drag ratios must exist for each section of the blade. Given the lack of this information for the FFA profiles, which are used in this blade, a simulation has been used for this purpose. The wind turbine blade profile has both a longitudinal rotation and the shape of its profile changes too. Hence, it is necessary to cut the cross section in different directions and examine the section profiles according to the existing standard profiles to obtain the general ratios of lift and drag of the blade. Figure 7 shows the blade profile with its sections.

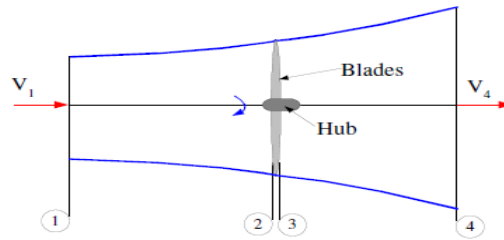


Figure 5: A view of the flow passing around the wind turbine

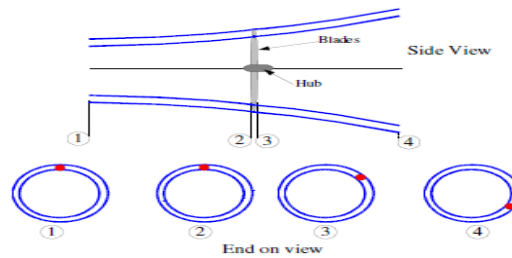


Figure 6: A view of the rotating circular flow around the blade plate

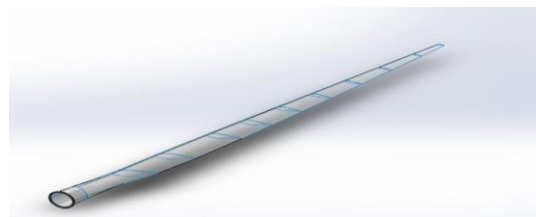
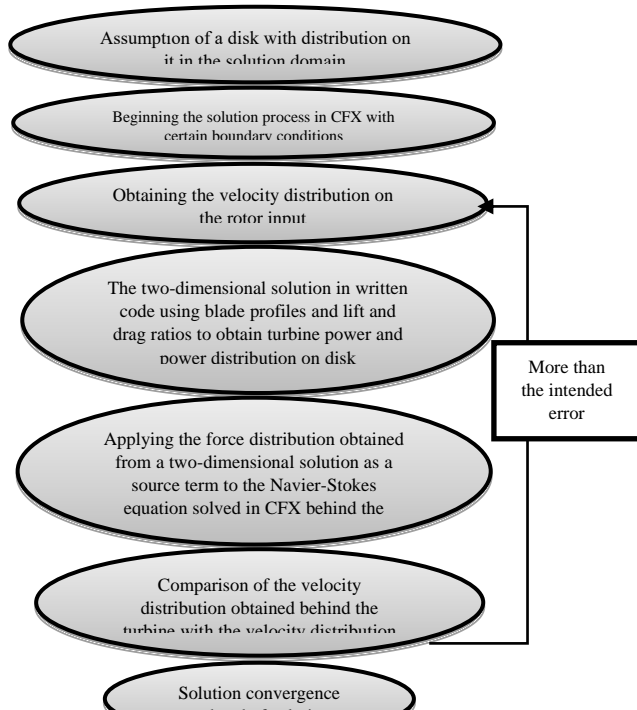
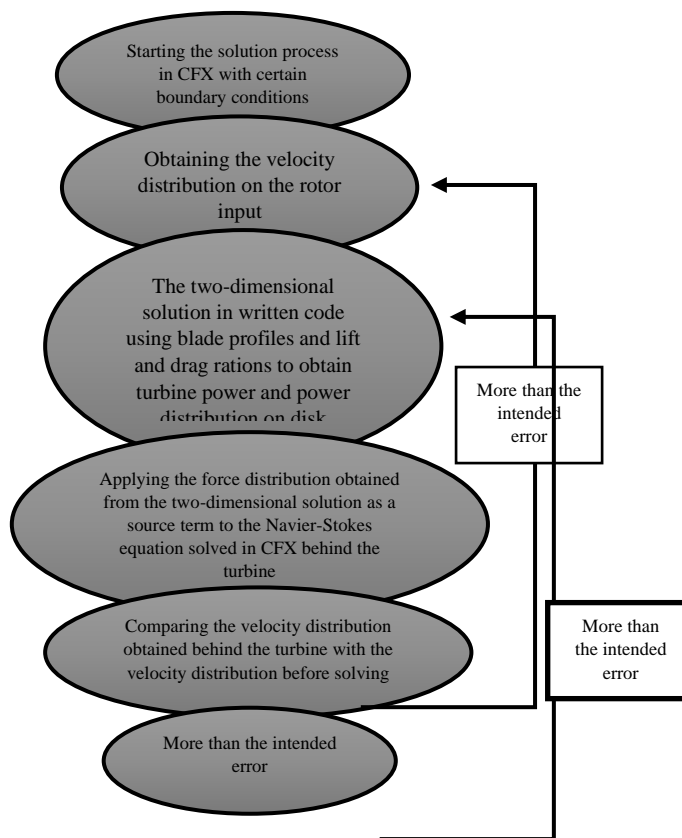


Figure 7: Profiles of the various sections of wind turbine blades





**Figure 8:** Algorithm for solving BEM

### 3. RESULTS

For accurate study of the flow around the profiles of different wind turbine sections and examining the presence or absence of separation phenomenon in wind turbine sections, the relative velocity vector for various radii is shown in Figure 9. As is seen, there is no separation at any of the stages indicating that the wind turbine is working in the right conditions. The figure shows the velocity contour on the pressure surface (front) and the suction surface (back). As is seen, the greatest pressure is formed on the pressure surface as the point of stagnation occurs there. Moreover, the lowest pressure is applied to the suction surface because, as Figure 10 shows, the wind flow reaches a high velocity shortly after the point of rest and on the suction surface. Studying the pressure on the suction surface shows that the farther we get from the edge of the attack and closer to the edge of escape, the more it increases. The axial velocity contour on the plane passing through the middle of the solution domain ( $x = 0$ ) is shown in Figure 11. The flow wake area behind the turbine, where the flow velocity is less than the wind flow velocity, is clearly visible. It has to be noted that this area has to be eliminated after the turbine and not reach the boundaries of the system, as the boundary conditions will be wrong in this case. This is well seen in the figure. The axial velocity contours at different distances from the center of the vanes are shown in Figure 12 to accurately study the flow area behind the turbine more. The comparison of

the axial velocity at various distances shows that the farther we go from the wind turbine, the lower and maximum velocities decrease. However, as already stated, the rate of uniformity of velocity behind the wind turbine is very slow. Moreover, it is clear that there are three regions with lower axial velocities than the other points in each of these shapes, located approximately in the middle radius of the blades. Now, in the last step, the wind turbines must be analyzed and examined together and the output power of these wind turbines can be obtained at different distances from each other. It has to be stated that if the distance of wind turbines in a wind farm is short, the presence of wake and whirlpools of the turbines in the front row turbines will have a negative effect on the rear row turbines and the output power of wind turbines will reduce. Furthermore, if the distance between wind turbines in a wind farm is large, the output power of the turbines will not reduce, but a lot of land will be occupied for the installation of turbines, which is naturally not economically viable. Thus, the optimal distance for wind turbines in a wind farm has to be sought so that besides the maximum output power of wind turbines, not much land is used to install these turbines. According to the results obtained from the application of mathematical equations and BEM method and the results of numerical analysis by CFX software, we reach the numbers in Table 2. Indeed, nine longitudinal and transverse distances that back-row turbines can have with other wind turbines in the optimal state are presented in Table 2, and numerical analysis has been performed for all these distances. It has to be stated that the optimization was done in these longitudinal and transverse distances mentioned, the output power of wind turbines to reach its maximum value and at the same time the minimum land used to install wind turbines should be considered. It is critical to note that all of these 9 distances presented in Table 2 are optimal, but if it is necessary to consider a longitudinal and transverse distance as the optimal point, the axial distance is 5 times the rotor diameter ( $5D$ ) and the transverse distance is three. Equivalent distance equal to the rotor diameter ( $3D$ ) can be considered. This is because while the output power of wind turbines at this distance is desirable, it has the least space occupied among these 9 proposed axial and transverse distances. Thus, only the axial and transverse distances are shown in Figure 13 as the optimal distance. Moreover, it has to be stated that the numbers listed in Table 2 refer to back-row turbines, because the front-row turbine (in this study, there is one front-row turbine and two rear-row turbines) receives wind flow at the main velocity without any obstruction and the only problem is the back-row wind turbine. It has to be noted that the diameter of the wind turbine rotor analyzed in this study (V-47 660KW) is 47 meters. As Figure 13 shows, these distances have not adversely affected the rear-row wind turbine. The solution field must be considered to examine this. The velocity field for the axial distance mode is 5 times the rotor diameter ( $5D$ ) and the transverse distance 3 times the rotor diameter ( $3D$ ) as shown in Figure 13. It is seen that the third turbine is not yet located behind the first turbines and still receives the wind flow at the main velocity. Thus, it can generate power with the same initial capacity. The figure shows that the flow enters the first row turbines at a certain velocity from the input boundary. Because of using wind energy, as stated in the two-dimensional method, a resistive force is generated in the rotor

that reduces the velocity at which the turbine enters. Thus, a small flow is diverted around the rotor and reaches its maximum divergence at a distance of ten times the diameter of the rotor. After this process, the flow shrinks in the front part. Given the large lateral distance and the short longitudinal distance, the third turbine is not placed in the wake of the first turbine and as is seen, high velocity flow is available to this turbine and its power is not reduced. It must be noted that this layout was done for 3 turbines and other wind turbines must be placed in the same way and with the same layout.

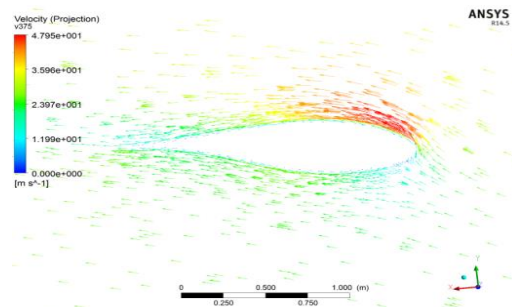


**Figure 9:** Relative velocity vector of wind turbine blade at  $r / R = 0.375$

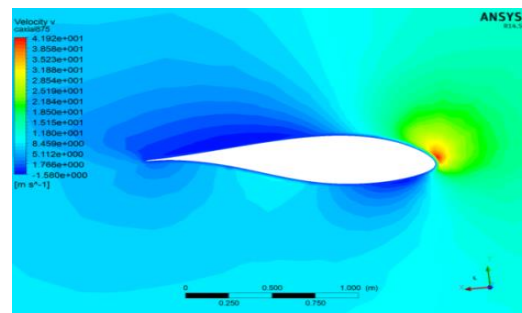


**Figure 10:** Axial velocity contour of wind turbine blade  $r / R = 0.375$

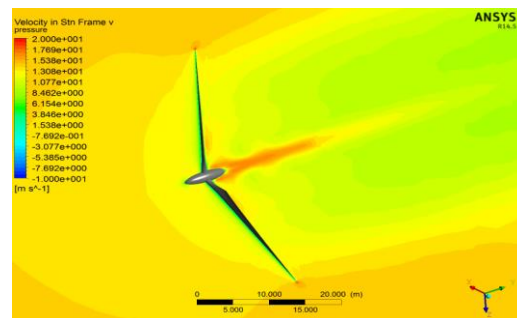
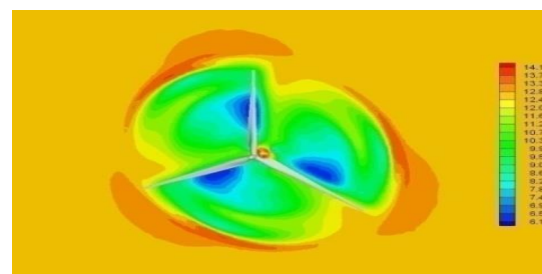


**Figure 11:** V-47 660 KW wind turbine axial velocity counter



**A**

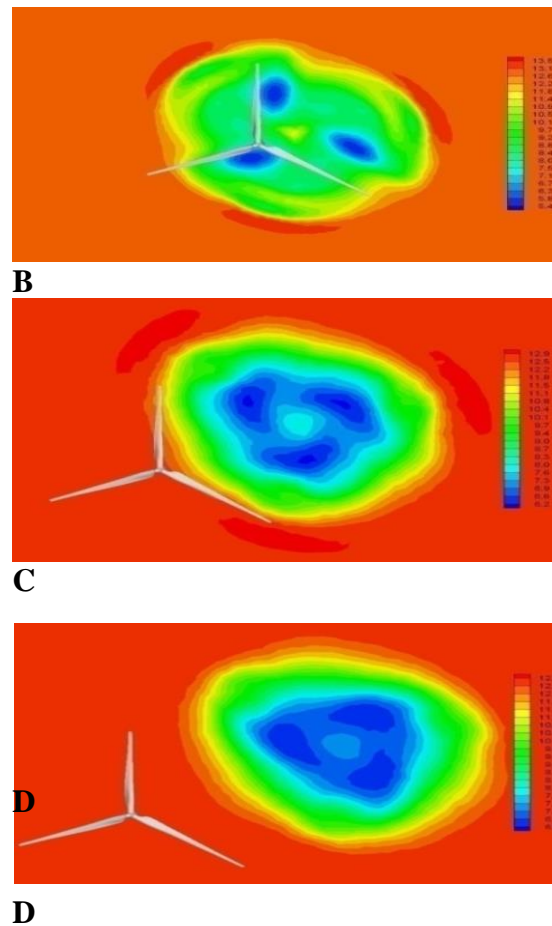


**Figure 12:** Axial velocity contour at various distances from V-47 660 KW wind turbine

(A)  $y / R = 0.125$ , (b)  $y / R = 0.5$ , (c)  $y / R = 1$  (t)  $y / R = 2$

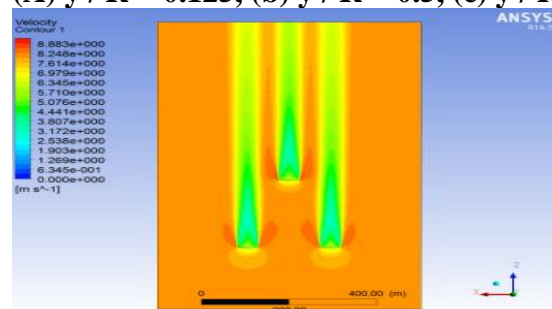


**Figure 13:** Velocity counter for 3 wind turbines in the wind farm

**Table 2:** Power output of back row turbines in various layouts in terms of kilowatts

Axial distance / transverse distance	3D	4D	5D
5D	706	701	706
6D	698	701	706

7D	690	700	706
----	-----	-----	-----

#### 4. Conclusion

The purpose of the study was to provide the best layout of large size wind turbines in the wind farm, so that the highest efficiency can be obtained from wind turbines or in other words, the wind turbines generate the most electricity. In the study, first a single wind turbine was examined and the flow-conditions before and after applying this wind turbine were examined. Then the three wind turbines were examined together. It has to be noted that this study was done numerically in CFX software. Furthermore, the study used BEM, where BEM theory was used for aerodynamic calculations of wind turbine blades. Overall, this theory can be used for aerodynamic analysis of wind turbine blades or its design from scratch. Another advantage of using BEM is reducing the number of elements and meshes in the numerical model, resulting in the reduced problem-solving time. Finally, based on the analyses of a single wind turbine and then the three wind turbines in the wind farm, the most optimal axial and transverse distances the wind turbines should have relative to each other were obtained and listed in Table 2. Table 2 shows the 9 longitudinal and transverse distances that back-row wind turbines can have with other wind turbines in the optimal condition, for all of which numerical analysis was performed. It has to be noted that the purpose of optimization is the output power of wind turbines reaching their maximum value at these longitudinal and transverse distances and the minimum land being used to install wind turbines at the same time. All 9 axial and transverse distances stated in Table 2 are optimal, but if one has to name one axial distance and one transverse distance as optimal distances, the axial distance 5 times the rotor diameter (5D) and the transverse distance 3 times the rotor diameter (3D) are the optimal distances. This is because while wind turbine output power is maximum, less space is used to install wind turbines.

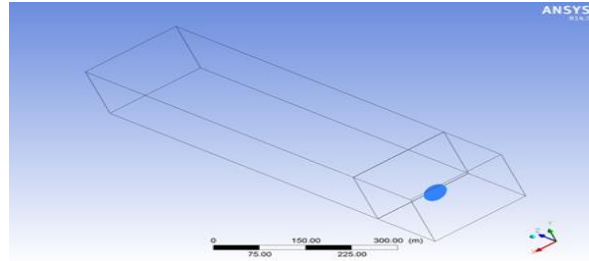
#### Validation

A 660 kW experimental wind turbine manufactured by Saba Niroo Co. [9] has been numerically modeled with its output power compared with the associated experimental model to validate the numerical results obtained in the study. Comparison of the results related to the output power of the experimental wind turbine provided by Saba Niroo Co. [9] and the output power of the numerical wind turbine shows that this numerical study is acceptable in terms of accuracy. As is seen, the results are highly in line with the experimental measurements up to 8.5 m/s. The existing error could be due to the fact that at higher velocities, the turbine control screw system seems to be activated and the blade angle is changed given the change in the trend of the diagram. It shows more power, as the blade angle has been kept constant in the simulations.

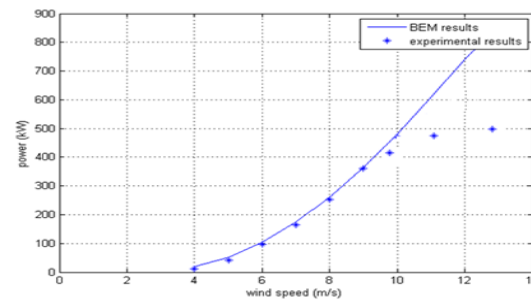
It has to be borne in mind that the role of the control system is to reduce the power at high velocities so that the nominal power tolerable by the components does not increase. Thus, the difference in the diagrams at high velocities is quite natural (Figure 14).



A [9]



B



C

**Figure 14:** Experimentally and numerically modeled V-47 660 KW wind turbine

A) Experimental wind turbine KW V-47 660 by Saba Niroo Co. [8], b) Numerical solution range of wind turbine KW V-47 660, c) Comparison of the output power of experimental and numerical wind turbine obtained by BEM

**ACKNOWLEDGMENT**

Hereby, I feel obliged to thank my dear professors. The research supervised by these professors and the lessons learned from these great people enabled me to learn the way and method of research and teaching besides valuable scientific topics. Moreover, my special gratitude to my dear parent, whose presence is a blessing to me and names a proof of my being whose unwavering assistance during my studies will never be forgotten. I hope that the study has compensated a small part of their love.

**Symbols**

Rotor radius (m)	R
Rotor velocity (m / s)	V
Wind turbine power (KW)	P

Wind density (kg / m <sup>3</sup> )	$\rho$
Axial induction coefficient (without unit)	$a$
Blade cross-section (m <sup>2</sup> )	$A$
Blade correction factor (without unit)	$Q$
Momentum coefficient (without unit)	$\Omega$
Angle of attack (°)	$\beta$

## REFERENCES

- Cal, Ra., Ramos, A.N., Hamilton, N., Houck, D., Spacing dependence on wind turbine array boundary, 17th International Symposium on Applications of Laser Techniques to Fluid Mechanics Lisbon. Lisbon, Portugal, pp. 07-10, 2014. *Strength of Materials*, Vol. 48, No. 1, pp. 127-134, 2016.
- Gones, G., Bouamane, L., "Historical trajectories and corporate competences in wind energy". Harvard Business School Entrepreneurial Management Working Paper. Vol. 4, No. 11-112, 2011.
- Jan, B., Wake Measurements Behind An Array Of Two Model Wind Turbines. KTH School of Industrial Engineering and Management Energy Technology EGI-2011-127 MSC EKV 866 Division of Heat and Power Technology SE-100 44 STOCKHOLM, October 31st, 2011.
- D'Ambrosio, M., Medaglia, M., Vertical Axis Wind Turbines: History, Technology and Applications. Master thesis in Energy Engineering, pp. 3-18, May 2010.
- Wind Turbine Blade Design Optimization, Anonymous MIT Students. Massachusetts Institute of Technology, Cambridge, MA, 02139, USA, April 2010.
- Mansour, K., Yahyazade, M., "Effects of turbulence model in computational fluid dynamics of horizontal axis wind turbine aerodynamic". *WSEAS Trans. Appl. Theor. Mech.* Vol. 3, No. 6, 2011.
- Wu, T., Porté-Agel, F., "Atmospheric turbulence effects on wind-turbine wakes: An LES study". *Energies*, Vol. 5, No. 12, pp. 5340-62, Dec 2012. doi:10.3390/en5125340, 2012.
- Hsiao, F.-B.; Bai, C.-J.; Chong, W.-T. The Performance Test of Three Different Horizontal Axis Wind Turbine (HAWT) Blade Shapes Using Experimental and Numerical Methods. *Energies* 2013, 6, 2784-2803. <https://doi.org/10.3390/en6062784>
- Saba Niroo Co. affiliated to Sadid Industrial Group, [www.sabaniroo.co.ir](http://www.sabaniroo.co.ir)